2014 IEEE International Conference on Robotics & Automation (ICRA)
Hong Kong Convention and Exhibition Center
May 31 - June 7, 2014. Hong Kong, China

Shape Prediction Algorithm for Flexible Endoscope

Jiun Jeon and Byung-Ju Yi, *Member, IEEE*

Abstract— **Flexible endoscope has been used for the diagnosis of the large intestine. This paper aims at the development of navigation software that provides the surgeon with the 2D/3D shape of flexible endoscope inside the colon real time. It helps surgeon insert the endoscope in a safe manner and locate the position of the lesion. With the information of the insertion length and the position/orientation information of the distal end, we propose a shape prediction algorithm with consideration of constrained geometry and gravity load of the flexible endoscope. To corroborate the effectiveness of the shape prediction algorithm, we perform simulation using 2D/3D flexible endoscope models and verify the result through experiments.**

I. INTRODUCTION

Medical care can be classified as diagnosis and therapy. In the medical therapy, surgical robots have drawn much attention. Successful commercialized products are being used in clinics. In the medical diagnosis, many devices such as MRI, CT and ultrasonic device are indispensable in hospitals. Moreover, a variety of navigation software based on patient data obtained from those diagnosis devices are being used in clinics. These days, efforts to combine the diagnosis tools and surgical robots are being pursued all over the world.

However, currently existing navigation software still needs to enhance reliability and operational accuracy for extensive usage in clinics. High performance navigation software would minimize the usage of diagnosis device in the intra-operative procedure. As a result, exposure to radiation and operation time could be reduced.

Advent of the endoscope has changed the paradigm of surgery greatly. Even narrow spaces inside the human body could be visualized using the endoscope. Specially, flexible endoscope is a good means to diagnosis the internal states of the stomach or the colon. However, just looking at the camera image, it is hard for surgeon to recognize the direction and location of the distal end of the flexible endoscope inside the colon. Though continual usage of X-ray may help recognize the current states, it is not recommended because of too much radiation exposure and inconvenience of installing the C-arm during diagnosis.

Continuum type robot manipulators have drawn much attention these days. Different from industrial robot manipulators being used in automation fields, continuum type robot systems are useful for applications such as exploration of curved environment like pipelines or sinus of the human body. Biomimetic robotic systems mimicking the legs of mollusks such as a continuum-like octopus have been also a rising research field. Quite a few research works on kinematic modeling of continuum kinematic chains have been reported [1-4]. Applications of continuum kinematic chain also have been very diverse [5-6]. The transmission line of the colonoscope is also a kind of continuum. It is a continuous system, so it is usually hard to predict the behavior in the free space. Such a continuum kinematic chain can be modeled as a kinematically redundant robot manipulator which has more joint inputs compared to the number of output [7-8]. Other researchers modeled the continuum as an elastic kinematic chain [9-11] .

Shah, et al [12-13] investigated the shape prediction algorithm for colonoscope. They reported successful data in the clinical application. However, attaching multiple electromagnetic sensors on the surface of flexible endoscope makes it hard to insert it into the patient's colon because of many wires and sensors around the flexible body. Possible infection is another problem.

In this paper, we propose a shape prediction algorithm of the flexible colonoscope based on the information of only one electromagnetic sensor and the insertion length of the flexible body. For this, we model the colonoscope as an elastic kinematic chain having abundant joints and links. In other words, it is modeled as a kinematically-redundant system. Using this model, the shape prediction algorithm of the colonoscope is suggested for the given boundary condition. Numerical simulation is conducted to estimate the motion behavior of the elastic colonoscopy and experimental work is also performed to corroborate the effectiveness of the proposed algorithm.

The procedure of this paper is as follows. In section II, 2D and 3D modeling of flexible continuum is introduced. Specifically, the flexible continuum used for the endoscope is modeled as a continuous spring wire since it possesses a coil spring inside the flexible body. In contrast to models of other continuum mechanisms of small size, we include the gravity load in the modeling of the flexible continuum. Using this model, we perform numerical simulation of the flexible continuum in section III. In order to verify the simulation result, we perform experiments in section IV. Finally, we draw conclusion.

II. MODELING OF ELASTIC KINEMATIC CHAINS

A. Continuum Modeling in 2-dimension

We assume that the 2D continuum model of Fig. 1 belongs to $W = R^2$ and that it has infinite number of joints (at least $N \geq 3$, where N is the number of links).

The output coordinate of the $(i+1)$ -*th* link can be expressed as a recursive form given by

Jiun Jeon is with the Electronic Systems Engineering Department, Hanyang University, Ansan, Korea (e-mail:jiun@hanyang.ac.kr).

B.- J. Yi is with the Electronic Systems Engineering Department, Hanyang University, Ansan, Korea (corresponding author, e-mail: bj@hanyang.ac.kr).

$$x(i+1)=\begin{bmatrix} x_{i+1} \\ y_{i+1} \\ \theta_{i+1} \end{bmatrix} = x(i)+\begin{bmatrix} r_i\cos\theta_i \\ r_i\sin\theta_i \\ \phi_i \end{bmatrix}, \quad (1)$$

where r_i is the link length of the i -*th* module.

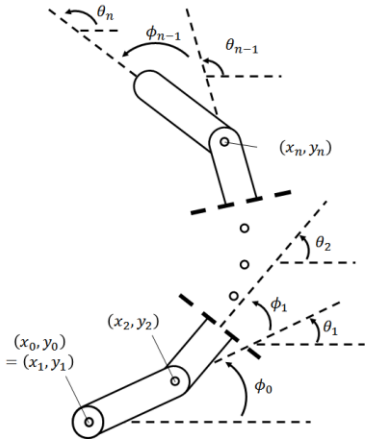

Fig. 1. 2D Model of continuum

In fact, a torsional spring is embedded inside the serial structure of colonoscopy. Therefore, we can model the colonoscopy as an elastic kinematic chain. Modeling the colonoscopy as N-lumped bodies, the potential energy of the i -*th* module is given by

$$P_E(i)=\frac{1}{2}k_i\phi_i^2, \quad (2)$$

where k_i and ϕ_i are the stiffness of the i -*th* module and the relative joint angle of the i -*th* joint, respectively.

Then, the shape of the elastic kinematic chain will be formed in such a way to minimize the total potential energy of the N-moduled continuum. Thus, the optimization problem can be defined as

$$\text{Minimize} \sum_{i=0}^{N} P_E(i)$$

$$\text{subject to } x(i+1)=x(i)+\begin{bmatrix} r\cos\theta_i \\ r\sin\theta_i \\ \phi_i \end{bmatrix} \text{ for all } i \in \{0,\ldots,n\} \quad (3)$$

$$x(0)=0 \;\&\; x(N)=b \text{ for some } b \in W$$

B. Continuum Modeling in 3-Dimension

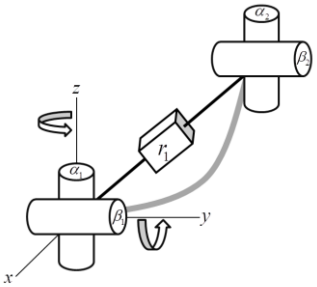

Fig. 2. Modeling of one module in 3D

In the 3-dimensional workspace, each module (link) of the continuum kinematic chain can be modeled as Fig. 2, which is composed of two universal joints and a link connecting them. The output space of the continuum kinematic chain belongs to $W=R^6$. For redundancy, the continuum kinematic chain should have more than 3 links and 6 joints ($2N \geq 6$).

The output of the (i +1)-*th* module of the continuum kinematic chain is denoted as

$$x(i+1)=\begin{bmatrix} \mathbf{P}_{i+1} \\ \mathbf{\Omega}_{i+1} \end{bmatrix}. \quad (4)$$

In (4), $\mathbf{P}_{i+1}$ is the position vector of the (i +1)-*th* link and it is expressed as a recursive form given by

$$\mathbf{P}_{i+1}=\begin{bmatrix} x_{i+1} \\ y_{i+1} \\ z_{i+1} \end{bmatrix} = \mathbf{P}_i + \mathbf{R}_i \bullet {}^i\mathbf{R}_{i+1} \begin{bmatrix} r_{i+1} \\ 0 \\ 0 \end{bmatrix}, \quad (5)$$

where

$${}^i\mathbf{R}_{i+1}=\begin{bmatrix} \cos\alpha_i\cos\beta_i & -\sin\alpha_i & \cos\alpha_i\sin\beta_i \\ \sin\alpha_i\cos\beta_i & \cos\alpha_i & \sin\alpha_i\sin\beta_i \\ -\sin\beta_i & 0 & \cos\beta_i \end{bmatrix}. \quad (6)$$

In (5), $\mathbf{R}_i$ is the rotation matrix of the *i-th* coordinate frame relative to the global frame and ${}^i\mathbf{R}_{i+1}$ is the rotation matrix of the $(i+1)$ -*th* frame relative to the (i)-*th* frame, respectively. In (4), $\mathbf{\Omega}_{i+1}$ is the orientation vector, which is defined by three (Z-Y-X) Euler angles (α,β,γ). The components of $\mathbf{\Omega}_{i+1}$ given by

$$\mathbf{\Omega}_{i+1}=\begin{bmatrix} \alpha_{i+1} & \beta_{i+1} & \gamma_{i+1} \end{bmatrix}^T \quad (7)$$

are obtained by using $\mathbf{R}_i \bullet {}^i\mathbf{R}_{i+1}$.

In the 3-dimensional space, we can define a bending plane as Fig. 3 and the bent angle γ between two solid lines can be obtained from the geometry where the angles of the universal joint connecting two links are given as α and β. Then, the potential energy due to deflection of the continuum kinematic chain can be defined as

$$P_E(i)=\frac{1}{2}k_i\gamma_i^2+m_igz_i, \quad (8)$$

where $\gamma_i=\cos^{-1}(\cos\alpha_i\cos\beta_i)$, m_i is the mass of the i -*th* link, g is the gravity constant, and z_i is the height of the i -*th* module.

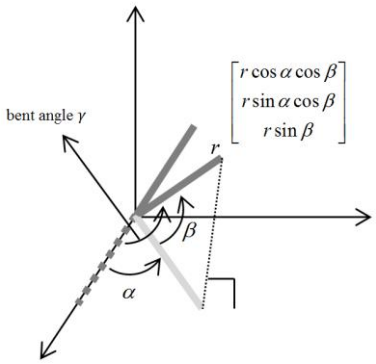

Fig. 3. The bending plane

C. *Secondary Criteria Optimizing Potential Energy of the System*

Yoshikawa [7-8] proposed redundancy resolution algorithms. Using the homogeneous space, the given performance criterion can be optimized. In the 2-dimensional space, the performance criterion denoting the total potential energy is expressed as

$$p = \sum_{i=0}^{N} P_E(i) = \frac{1}{2}\sum_{i=0}^{N} k_i \phi_i^2. \tag{9}$$

Differentiating (9) with respect to time gives

$$\dot{p} = \sum_{i=0}^{N} k_i \phi_i \dot{\phi}_i = \mathbf{B}\dot{\Phi}, \tag{10}$$

where $\mathbf{B} = \begin{bmatrix} k_0\phi_0 & \cdots & k_N\phi_N \end{bmatrix}$ and $\dot{\Phi} = \begin{bmatrix} \dot{\phi}_0 & \cdots & \dot{\phi}_N \end{bmatrix}^T$.

In the 3-dimensional space, the performance criterion is given by

$$p = \sum_{i=0}^{N} P_E(i) = \sum_{i=0}^{N}\left(\frac{1}{2}k_i\gamma_i^2 + m_i g z_i\right). \tag{11}$$

Differentiating (11) with respect to time gives

$$\dot{p} = \sum_{i=0}^{N}\left(k_i\gamma_i\dot{\gamma}_i + mg\dot{z}_i\right) = \mathbf{B}\dot{\Phi} = \mathbf{B}\begin{bmatrix}[\dot{\boldsymbol{\alpha}}] \\ [\dot{\boldsymbol{\beta}}]\end{bmatrix}, \tag{12}$$

where

$$\mathbf{B} = \begin{bmatrix}\mathbf{B_1} & \mathbf{B_2}\end{bmatrix}, \tag{13}$$

$$\mathbf{B_1} = \begin{bmatrix} \dfrac{\cos^{-1}(\cos\alpha_0\cos\beta_0)}{\sqrt{1-\cos^2\alpha_0\cos^2\beta_0}}k_0\sin\alpha_0\cos\beta_0 + m_i g\dfrac{\delta z_0}{\delta\alpha_0} \\ \vdots \\ \dfrac{\cos^{-1}(\cos\alpha_n\cos\beta_n)}{\sqrt{1-\cos^2\alpha_n\cos^2\beta_n}}k_n\sin\alpha_n\cos\beta_n + m_i g\dfrac{\delta z_n}{\delta\alpha_n} \end{bmatrix}^T, \tag{14}$$

and

$$\mathbf{B_2} = \begin{bmatrix} \dfrac{\cos^{-1}(\cos\alpha_0\cos\beta_0)}{\sqrt{1-\cos^2\alpha_0\cos^2\beta_0}}k_0\cos\alpha_0\sin\beta_0 + m_i g\dfrac{\delta z_0}{\delta\beta_0} \\ \vdots \\ \dfrac{\cos^{-1}(\cos\alpha_n\cos\beta_n)}{\sqrt{1-\cos^2\alpha_n\cos^2\beta_n}}k_n\cos\alpha_n\sin\beta_n + m_i g\dfrac{\delta z_n}{\delta\beta_n} \end{bmatrix}^T. \tag{15}$$

The following steps are commonly applied irrespective of the dimension. The equation that relates the output x to the input Φ is given by

$$x = f(\Phi). \tag{16}$$

Differentiating (16) with respect to time yields

$$\dot{x} = J\dot{\Phi}. \tag{17}$$

Inverting (17), the solution of (17) is obtained as

$$\dot{\Phi} = J^{+}\dot{x} + (I - J^{+}J)\varepsilon, \tag{18}$$

where $J^{+} = J^T(JJ^T)^{-1}$ denotes the pseudo-inverse of J.

The second term of (18) denotes the null-space which creates a self-motion inside the joint space. An arbitrary constant vector $\varepsilon \in R^{2N}$ is decided to optimize some criterion.

Substituting (18) into (12), we have

$$\dot{p} = \mathbf{B}J^{+}\dot{x} + \mathbf{B}(I - J^{+}J)\varepsilon. \tag{19}$$

If we propose to select ε as

$$\varepsilon = \mathbf{B}^T\varepsilon_1, \tag{20}$$

where ε_1 is a constant. Hence we obtain

$$\dot{p} = \mathbf{B}J^{+}\dot{x} + \mathbf{B}(I - J^{+}J)\mathbf{B}^T\varepsilon_1, \tag{21}$$

where if we set ε_1 as a negative value, the second term in the right-hand side of (21) becomes nonnegative due to the fact that $\mathbf{B}(I - J^{+}J)\mathbf{B}^T$ is non-negative, contributing to an decrease of the value p (minimize the total potential energies).

Integrating (18) with respect to time, we can obtain the joint angles and are able to draw the shape of the colonoscope.

III. SIMULATION

A. *2D simulation*

First of all, we perform some basic 2D simulations to show how the shape prediction algorithm works for elastic kinematic chain. The elastic kinematic chain is modeled as having 10 joints and 10 links. Fig. 4 demonstrates that the initial input state transits to the final state in such a way to minimize the potential energy of the system. It is noted from Fig. 5 that the total potential energy of the system converges to a constant value. Fig. 6 also demonstrates different shapes of the elastic kinematic chain according to different output boundary conditions (position and orientation of the end point).

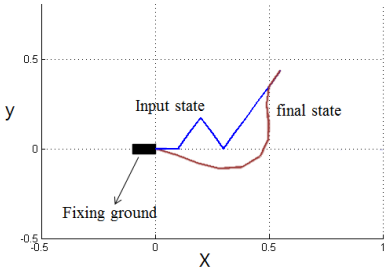

Fig. 4. Shape transition of the elastic kinematic chain

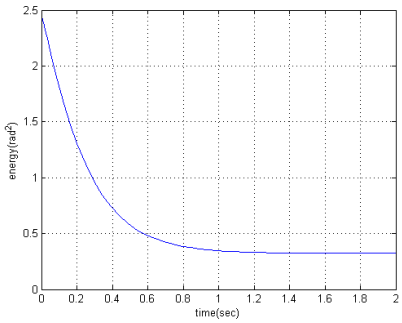

Fig. 5. Potential energy of the system

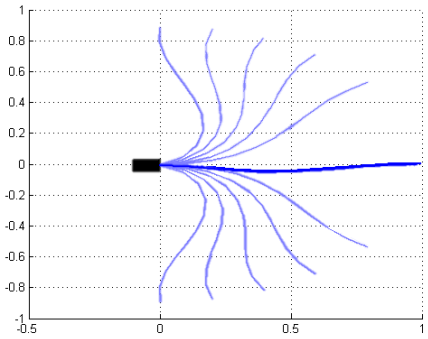

Fig. 6. The shapes with respect to output boundary conditions

B. *Simulation for constrained case*

Fig. 7 denotes the X-ray image of a flexible endoscope, which is taken during colonoscopy. It is observed that the flexible endoscope is constrained to the left and right walls and peritoneum. Thus it is necessary to consider the anatomical constraint for precise shape prediction. To our knowledge, there is no prior work that deals with shape prediction with consideration of the anatomical constraint as shown in Fig. 7.

Fig. 7. X-ray image of the flexible endoscope.

As an initial study for this problem, we construct a test platform to deal with this problem. Fig. 8 shows comparison of simulation and experimental results for this case. The slim yellow line laid over the flexible body denotes the simulation result. In order to represent the simulation result, VTK (Visualization Tool Kit) was employed to visualize the shape. It is clearly shown that without reflecting the constrained geometry the simulation result of Fig. 8(a) is different from the shape of the endoscope. This is because the force exerted on the flexible body by the left wall was not modeled in the shape prediction algorithm. So it is necessary to measure the force distribution along the surface of the flexible body. However, this approach is not practical because it is hard to implement sensors on the surface of the flexible endoscope. Thus we adopt an indirect way. First of all, using the X-ray image of a patient, we can design the planar abdominal model of the patient. Using this information, the boundary of the endoscope can be estimated. Then we tune the stiffness of the continuum model. In the definition of potential energy of (11), the stiffness of each individual continuum module can be variable. In other words, if we set the stiffness of some continuum modules in the neighborhood of the contacting wall as very large values, the corresponding joints won't deflect much as a result of minimizing the potential energy. Thus, through this kind of post-processing, we could reshape the simulation result almost identical to the experimental result as shown in Fig. 8(b).

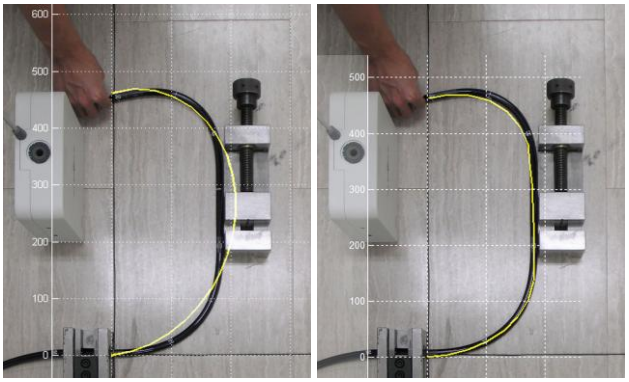

(a) without modification algorithm (b) with modification algorithm

Fig. 8. Reshaping the simulation result by including the wall model.

IV. Experimental Work

In order to corroborate the simulation result, we conducted experimental work. Aurora, which is an Electromagnetic Tracking System (EMTS), was employed to predict the shape of the colonoscopy. For experiment, we set up the test environment such that the proximal boundary condition is identical to the real colonoscopy inspection. The proximal end of the wire is clamped and fixed to a wall. For this experiment, we employ only two pieces of information: one electro-magnetic sensor and the inserted length of the flexible endoscope. The electromagnetic sensor returns three positions and three orientation of the distal end of the endoscope.

The same elastic wire used in colonoscopy whose length is 50cm was employed. One electromagnetic sensor is attached at the distal end of the flexible endoscope as shown in Fig. 9.

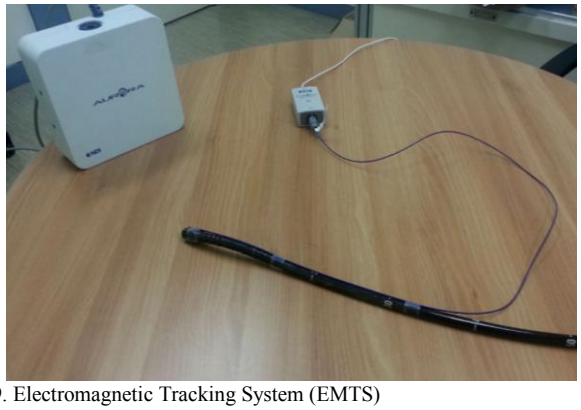

Fig. 9. Electromagnetic Tracking System (EMTS)

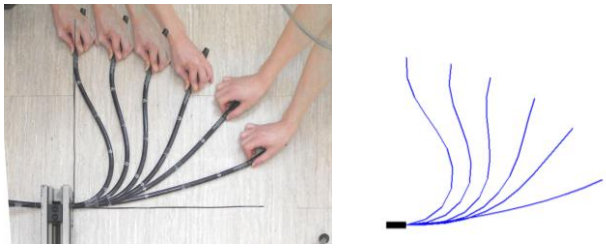

(a) Experimental result (b) Simulation result

Fig. 10. 2D wire prediction using electromagnetic tracking system

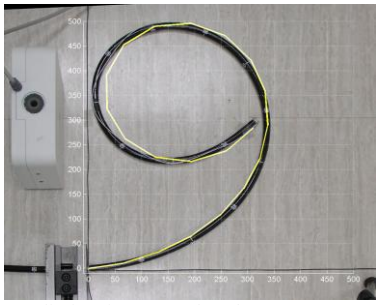

Fig. 11. 2D wire prediction for a complex shape

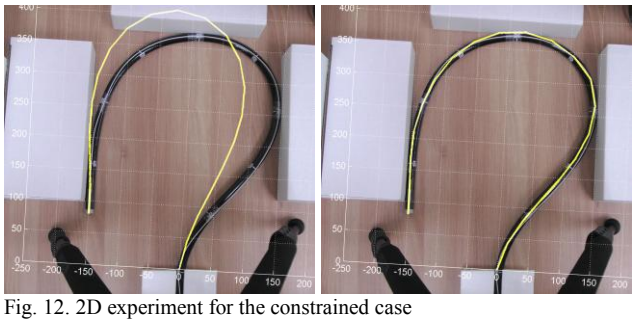

Fig. 12. 2D experiment for the constrained case

Fig. 10 and Fig. 11 denote comparison of simulation and experimental results. Even for a complex shape of the flexible endoscope, the shape prediction algorithm works very well. 2D experiment for the constrained case was also performed. It is noted from Fig. 12 that reshaping the stiffness model of the continuum modules in the neighborhood of the peritoneum, we could exactly match the simulation result to the experimental result.

In most motion estimation algorithms [9-11] of continuum mechanisms, the gravity effect has not been taken into account because of adapting the assumption of negligible weight of a small-sized continuum body. On the contrary, the flexible endoscope has considerable amount of weight, so the gravity load should be included in the shape prediction algorithm. In the 3D simulation, the continuum is modeled as having 8 links and 16 joints. Fig. 13(a) and Fig. 13(c) denote the shapes of the continuum without taking into account the gravity load in the potential energy model given by (11). However, when considering the gravity effect, it is clearly shown from the Fig. 13(b) and Fig. 13(d) that the simulation result is almost identical to the experimental result.

Thus, it is concluded that the proposed shape prediction algorithm is effective to estimate the shape of the colonoscope being inserted into the colon.

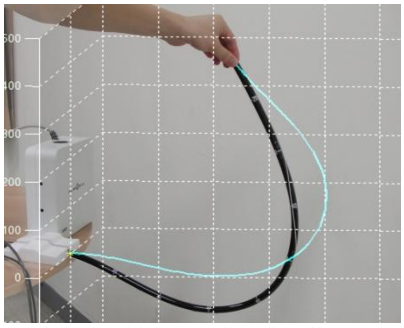

(a) without consideration of gravity effect (case 1)

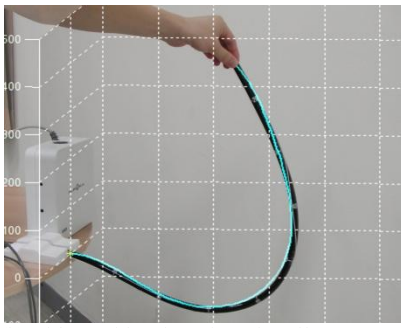

(b) with consideration of gravity effect (case 1)

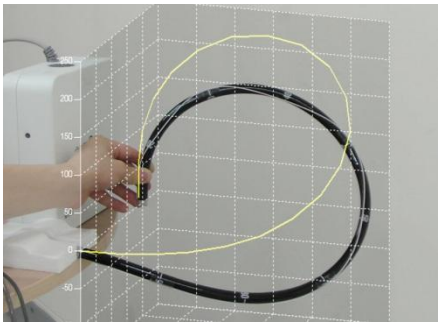

(c) without consideration of gravity effect (case 2 and 3)

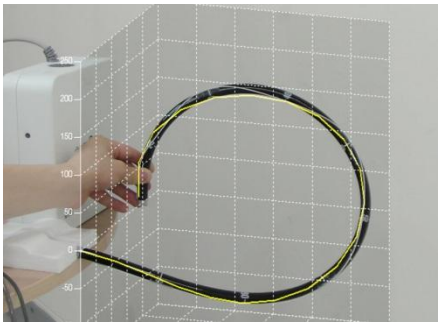

(d) with consideration of gravity effect (case 2 and 3)

Fig. 13. Comparison of simulation and experimental result for 3D case

V. CONCLUSION

The contribution of this paper is the shape prediction of colonoscopy which has the nature of elastic continuum. Given boundary conditions, the proposed optimization algorithm was able to predict the whole shape of the continuum both under constrained geometry and under gravity. Through experimental work, the feasibility of the proposed algorithm was verified. As a future work, the lumped continuum model

employed in this paper should be replaced by continuous continuum model which eventually minimizes the computation time and increase the accuracy of the shape prediction. Another future work is application of this shape prediction algorithm to real colonoscopy operation in the clinic.

ACKNOWLEDGEMENT

This work was supported by the BK21 Plus Program(Future-oriented innovative brain raising type, 22A20130012806) funded by the Ministry of Education(MOE, Korea) and National Research Foundation of Korea(NRF), supported by the Technology Innovation Program (10040097) funded by the Ministry of Trade, Industry and Energy Republic of Korea (MOTIE, Korea), supported by GRRC program of Gyeonggi Province (GRRC HANYANG 2013-A02), and financially supported by the Ministry of Trade, Industry and Energy (MOTIE) and Korea Institute for Advancement in Technology (KIAT) through the Workforce Development Program in Strategic Technology, supported by the MOTIE(The Ministry of Trade, Industry and Energy), Korea, under the Robotics-Specialized Education Consortium for Graduates support program supervised by the NIPA(National IT Industry Promotion Agency) (H1502-13-1001)

REFERENCES

[1] H.-S. Yoon, J. Jeon, J. H. Chung, and B.-J. Yi, "A Continuum module for developing a biopsy device," in *Proc. of Int. Conf. on Ubiquitous Robots and Ambient Intelligence*, pp. 442-444, 2012.

[2] H.-S. Yoon, S. M. Oh, J. H. Jeong, S. H. Lee, B.-J. Yi, K. Tae, and K.-C. Koh, "Active bending endoscope robot system for navigation through sinus area," *in Proc. of IEEE/RSJ Int. Conf. on Intelligent Robots and Systems*, pp. 967-972, 2011.

[3] D. B. Camarillo, C. F. Milne, C. R. Carlson, M. R. Zinn, and J. K. Salisbury, "Mechanics modeling of tendon-driven continuum manipulators," *IEEE Transactions on Robotics,* vol. 24, 2008, pp. 1262-1273.

[4] R. Jansen, K. Hauser, N. Chentanez, F. van der Stappen, and K. Goldberg, "Surgical retraction of non-uniform deformable layers of tissue: 2D robot grasping and path planning," *in Proc. of IEEE/RSJ Int. Conf. on Intelligent Robots and Systems,* pp. 4092-4097, 2009.

[5] M. W. Hannan and I. D. Walker, "Kinematics and the implementation of an elephant's trunk manipulator and other continuum style robots," *Journal of Robotic Systems,* vol. 20, 2003, p. 45-63.

[6] B. A. Jones and I. D. Walker, "Kinematics for multisection continuum robots," *IEEE Transactions on Robotics,* vol. 22, 2006, pp. 43-55.

[7] T. Yoshikawa, "Analysis and control of robot manipulators with redundancy," T*he first Int. symposium* in *Robotics research*, 1984, pp. 735-747.

[8] T. Yoshikawa, "Manipulability and redundancy control of robotic mechanisms," in *Proc. of IEEE Int. Conf. on Robotics and Automation*, 1985, pp. 1004-1009.

[9] T. Bretl and Z. McCarthy, "Equilibrium configurations of a kirchhoff elastic rod under quasi-static manipulation," in Proc. of *Workshop on Algorithmic Foundations of Robotics*, 2012.

[10] T. Bretl and Z. McCarthy, "Mechanics and quasi-static manipulation of planar elastic kinematic chains," *IEEE Transactions on Robotics,* vol. 29, 2013, pp. 1-14.

[11] D. Matthews and T. Bretl, "Experiments in quasi-static manipulation of a planar elastic rod," *in Proc. of IEEE/RSJ Int. Conf. on Intelligent Robots and Systems*, pp. 5420-5427, 2012.

[12] S. Shah, H. Pearson, S. Moss, E. Kweka, P. Jalal, and B. Saunders, "Magnetic endoscope imaging: a new technique for localizing colonic lesions," *Endoscopy*, vol. 34, 2002, pp. 900-904.

[13] S. G. Shah, B. P. Saunders, J. C. Brooker, and C. B. Williams, "Magnetic imaging of colonoscopy: an audit of looping, accuracy and ancillary maneuvers," *Gastrointestinal endoscopy*, vol. 52, 2000, pp. 1-8.